Squeezing lone pairs: The *A*17 to *A*7 pressure-induced phase transition in black phosphorus

Salah Eddine Boulfelfel,[1] Gotthard Seifert,[2] Yuri Grin,[3] and Stefano Leoni[2,*]
[1]*Stony Brook University, Department of Geosciences, New York 11794-2100, USA*
[2]*Technische Universität Dresden, Institut für Physikalische Chemie, D-01062 Dresden, Germany*
[3]*Max-Planck-Institut für Chemische Physik fester Stoffe, D-01187 Dresden, Germany*
(Received 30 November 2011; revised manuscript received 3 January 2012; published 18 January 2012)

We show how the ground state of phosphorus, black phosphorus, and the α-As type modification, next-lying on increasing pressure, are tightly connected over a Peierls intermediate. We unravel an intrinsic reactivity given by lone pairs, which are conserved during phase transition and are not suppressing the Peierls state. Along this line we provide a consistent solution to a classical chemical puzzle.

DOI: 10.1103/PhysRevB.85.014110 PACS number(s): 64.70.K−, 02.70.Ns, 71.15.Pd, 87.15.ap

I. INTRODUCTION

The polymorphism of the chemical elements is a complex topic of great experimental and theoretical interest. Extreme pressure and temperature conditions are promising setups for exotic crystal structures and properties. However, the reasons for the selection of a rather peculiar atomic pattern by a given element remain largely elusive. Even phosphorus, a classical element of the periodic system, remains surprising.[1,2] With three bonds and one lone pair, it is capable of a structural eclectism hardly attainable by other elements. Peculiar to this element is also the large number of still unsolved problems of its allotropy.[3–8]

Black phosphorus (space group *Cmca*, from now on *A*17) is a stable, semiconducting allotrope under ambient conditions.[9,10] Its crystal structure consists of corrugated layers of six-membered rings stacked along [001] (Fig. 1, left). Rings of three-connected phosphorus atoms in chair conformation share edges like in *cis*-decalin. Under moderate compression (∼5 GPa), black phosphorus transforms into the semimetallic arsenic-type structure (space group $R\bar{3}m$, from now on *A*7),[11] made of layers of six-membered rings linked in *trans*-decalin fashion instead (Fig. 1, right). This transformation between rather simple structures has repeatedly been considered over the years.[12–18] Preferential orientations obtained from diffraction experiments are used to validate structural transformation models based on symmetry reasonings.[17] While not group-subgroup related, *A*17 and *A*7 can be accommodated in a common monoclinic subgroup ($P2/c$) with phosphorus atoms on general Wyckoff positions ($4g$). They are interconverted by antiparallel displacements of adjacent (010) layers by $\pm 1/4$ along [100], coupled to a shear deformation decreasing the monoclinic angle β from 90° to 86.62°.

*A*17 and *A*7 can be derived from a simple cubic α-Po structure via a Peierls distortion.[19,20] The simple cubic structure is indeed adopted by phosphorus, however, at a much higher pressure (>12 GPa). Applying Woodward-Hoffmann rules to a monoclinic ($P2/m$) $A17 \rightarrow A7$ model based on distorting an underlying α-Po pattern, Burdett and Price found that bond reconstruction may be restricted to a single direction (along $[001]_{A17}$), like in the one-dimensional (1D) Peierls chain.[20] However, the concerted character of the process causes highest occupied molecular orbital (HOMO)/lowest unoccupied molecular orbital (LUMO) band crossing in orbital correlation diagrams,[20] which suggests a non-martensitic, discontinuous mechanism.

Characteristic of phosphorus are lone pairs, which are localized between corrugated layers in *A*17 and *A*7. Seo and Hoffmann[13] pointed out the absence of Fermi-surface nesting, expected in a truly Peierls system, due to *s*-*p* hybridization, which is responsible for lone pairs formation. While an active role of lone pairs can be expected,[21] this appears incompatible with a process driven by a Peierls distortion from an ideal simple cubic α-Po structure. However, are these true alternatives or is there a different, yet undisclosed way of combining Peierls distortion with lone pairs (strong *s*-*p* mixing[13])?

In this work, to answer this question we look for a novel picture of the transition mechanism. This entails working out an atomistic landscape that allows for a detailed understanding of local structural and electronic changes along the *A*7 to *A*17 transformation.

II. METHODS

Molecular dynamics (MD) is the method of choice for mechanistic investigations. However, the elucidation of transition paths suffers from a reduced efficiency, due to the presence of activation energy barriers. Transition path sampling (TPS)[22,23] MD was designed to cure this problem. Therein, an initial trajectory is iteratively driven toward a most probable trajectory regime, which represents the true transition. This is realized as a combination of molecular dynamics (MD) and Monte Carlo (MC) simulation steps.[22–25] In this approach the random walk is performed in the space of trajectories, instead of the space of configurations of a typical Monte Carlo simulation. A new path is generated from a previous one, requiring the forward move (old to new) to be exactly balanced by the reverse move, new to old.[23] The collection of the transition ensemble is ensured by the extensively used shooting algorithm. In the latter, the molecular-dynamics layer is used as a propagator. For a given trajectory, at a randomly chosen time slice small momentum perturbations are introduced, followed by propagation forward and backward in time. Provided the trajectory stays in the reactive regime of phase transition, the new trajectory is accepted with a probability proportional to the ratio of the distribution probabilities of the perturbed to the pristine time slice.[23] Otherwise a new perturbation move is made. Upon acceptance, the new trajectory becomes the old one, and the process is iterated.

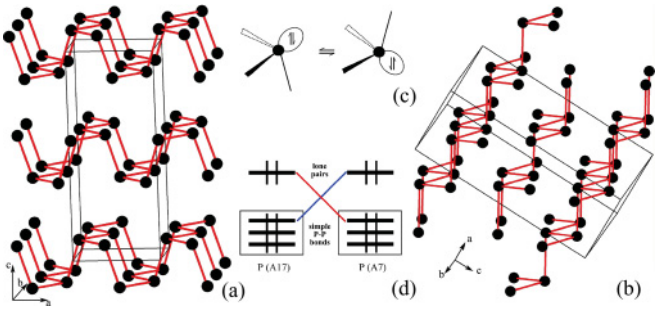

FIG. 1. (Color online) (a) Layered structure of black phosphorus ($A17$). (b) Corrugated layers of three-connected phosphorus in $A7$ type. (c) Cope-like rearrangement of tetrahedral phosphorus with repositioning of a lone pair. Orbital correlation diagram for the Woodward-Hoffmann-like rearrangement of $A17$ into $A7$ with crossing of states along the transformation path.

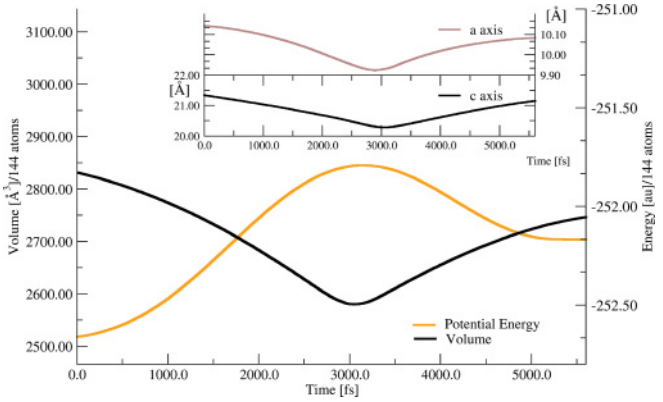

FIG. 2. (Color online) Averaged structural parameter and potential-energy changes [orange (gray) line] across the $A17$-$A7$ phase transition. Volume compression (black line) stabilizes $A7$. In the insets details on the c (layer stacking) and a axis variations are given. The zeroth time frame is arbitrarily set.

The simulation scheme requires an initial trajectory connecting the limiting structures. For this we have started the simulation from a path connecting $A17$ to $A7$, obtained from matching both structures in space group ($P2/c$) according to the monoclinic model described by Katzke and Tolédano.[17] The transposition of a geometric model into a first dynamic trajectory is achieved by selecting an intermediate configuration from the model, generating a velocity distribution at a given temperature, and propagating forward and backward in time, until either $A7$ or $A17$ are reached, respectively.[26]

TPS iterations were performed within the NPT (Ref. 27) ensemble ($p = 5$ GPa, $T = 300$ K) and implemented by applying momentum modifications on selected trajectory snapshots, keeping total energy, momentum, and angular momentum unchanged,[28] according to the shooting scheme.[23] Propagating the new configuration in both directions of time provides a new trajectory that is examined for the $A17$-$A7$ (or $A7$-$A17$) process, respectively. MD simulations were carried out using the density-functional tight-binding (DFTB), Γ point-only module of the CP2K package.[29] The accuracy of electronic density representation was checked against DFTB k-point calculations.[30] The time step $\Delta t = 0.2$ fs ensured a good time reversibility. Forces on phosphorus atoms were calculated using the DFTB method.[31] The mechanistic analysis is based on more than 100 transition pathways collected after trajectory convergence. The latter was inferred from the stability of the mechanistic features emerging during TPS MD. Different from the initial, concerted mechanistic models, the stable regime shows local events of bond nucleation and growth.

III. RESULTS AND DISCUSSION

In Fig. 2 ensemble averaged values of volume (black curve) and potential-energy [orange (gray) curve] changes across the $A17$-$A7$ phase transitions are plotted. A volume compression of approximately 3% from left to right can be appreciated. The potential-energy change amounts to ∼0.6 au/144 atoms cell (∼0.004 au/atom). The height of the energy barrier is 0.9 and 0.3 au, respectively. Noteworthy is the smooth volume variation from $t = 0$ to 2400 fs, and from 2600 to 5000 fs, with a rapid slope change in between. The c axis is pronouncedly shortened (layer compression), while the a axis is less affected (Fig. 2, inset). We now turn to the details of the reconstruction.

The structural reconstruction (Fig. 3) is commenced via antiparallel shuffling of corrugated (010) layers, without breaking the zigzag chains of P-P contacts along $[100]_{A17}$. At the same time the interlayer van der Waals space is squeezed out on the eve of the transformation, under cell parameter contraction in the $[001]_{A17}$ direction and shortening of P-P contacts. These atomic displacements, precursors to the $A17 \rightarrow A7$ transition are associated with the softening of B_{1g} and B^1_{3g} phonon modes[32,33] while the decrease of interlayer spacing closely reflects high-pressure experiments.[34]

Once P atoms are juxtaposed along $[001]_{A17}$ a new P-P contact is formed (Fig. 3, $t = 1240$). Subsequent bonds are highly correlated in the vertical direction (three to four bonds on the average, with less frequent five-bond sequences). This results in chains (Fig. 3, $t = 1740$, 1860 fs) that convert P

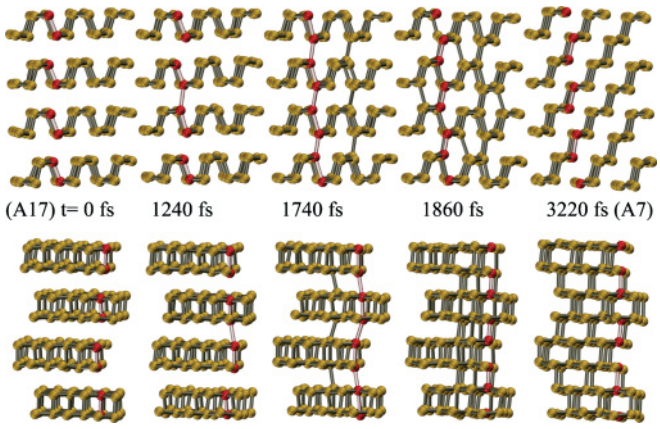

FIG. 3. (Color online) Mechanism for the $A17 \rightarrow A7$ transformation. Compression and layer shuffling of $A17$ ($t = 0$ fs) results in interlayer contacts ($t = 1240$ fs) and interlayer bonds ($t = 1740$–1860 fs), until reconstruction into $A7$ ($t = 3220$ fs). A vertical bond chain is highlighted ($t = 1740$ fs), and marked throughout. Upper row: orientation as in Fig. 1. Lower row: rotated by 90°. Zeroth time frame is set arbitrarily.

layers from *cis*- to *trans*-decalin under reorientation and restacking of the initial layers. The intermediate regime is characterized by the coexistence of *A*17 and *A*7 structural motifs (Fig. 3, $t = 1740$–1860 fs).

The process depicted in Fig. 3 is articulated over two different time scales: *slow* atomic movements ($\Delta t \sim 2000$ fs) on the one hand, which are associated with lattice deformations via layer shifts and cell compression, and *rapid* ($\Delta t \sim 120$–150 fs) bond flipping sequences along $[001]_{A17}$ on the other hand.

To visualize placement and changes of lone pairs along the transition the electron localizability indicator[35,36] (ELI) was evaluated[37] on a trajectory snapshot of *A*17 and *A*7 coexistence. ELI is a functional of same-spin electron pair density[35] and captures the local correlation of electronic motion in coordinate space. It can be computed[38] as the product of the electron density $\rho(\vec{r})$ and of the pair-volume function $\widetilde{V}_D(\vec{r})$, $\widetilde{\Upsilon} = \rho(\vec{r}) \cdot \widetilde{V}_D(\vec{r})$. $\widetilde{V}_D$ is proportional to the volume occupied by a fixed fraction of same spin electron pairs.[38] It is calculated from the Fermi hole curvature, $g(\vec{r})$,[36,39] as $\widetilde{V}_D(\vec{r}) = [\frac{12}{g(\vec{r})}]^{3/8}$. As for the electron localization function (ELF), ELI allows partitioning space into basins. Therein, charges can be integrated. For isolated atoms or core states, a shell structure appears. For molecules and solids, additional basins are formed, corresponding to chemical bonds and lone pairs. This feature is used here to characterize bonds and lone pairs, and to compute charges therein contained. An isoline representation of the resulting ELI map is given in Fig. 4.

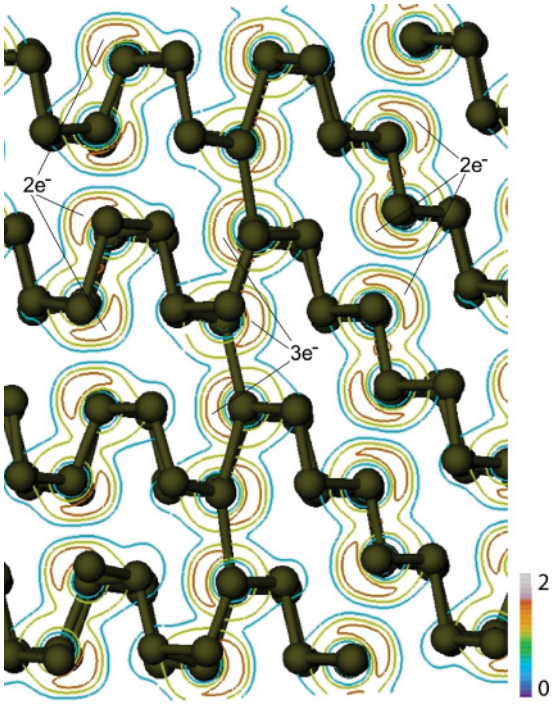

FIG. 4. (Color online) 2D cut (*a*,*c* plane) through the 3D ELI map. On the left- and rightmost parts (*A*17 and *A*7, respectively) lone pairs are visible ($\Upsilon = 1.5$). In the middle a chain is formed with sickle-shaped localization domains placed sideways. Lone pairs in *A*7 and *A*17 contain two electrons, while three electrons are found in the intermediate chain.

Three bond attractors (P-P) and one lone pair attractor are visible on P in both *A*17 and *A*7. Large localization domains ($\Upsilon = 1.5$) are found between layers, where lone pairs are expected from the valence shell electron pair repulsion (VSEPR) model.[21] In these ELI basins the electron density integrates up to two electrons.[40] The ELI map delimits pairs of P atoms forming P-P contacts both in the *A*17 (Fig. 4, left) and *A*7 (Fig. 4, right) structures. At the interface on the contrary, ELI isolines enframe a whole zigzag chain along $[001]_{A17}$. Therein, the former lone pairs lie sidewards of the chain in form of sickle-shaped localization domains containing three electrons. The extra electron results from the homolytic breaking of one P-P bond into P· ·P. Accordingly, the electron count obtained form ELI discloses an open-shell scenario with seven electrons for each P atom in the zigzag chain interfacing *A*17 and *A*7 structures (1 lone pair: 2 e^-, 2 intralayer P-P: 4 e^-, breaking of 1 P-P: 1 e^-). The process of formation of the intermediate chain can be described as a polymerization of P_2 units into a -$(P_2)_n$- polymer, which is accompanied by a sudden change of P-P contacts along $[001]_{A17}$, in the form of a vertical crack in Fig. 4. The ELI map and electron count indicate that the chain is the exact halfway point on the process of breaking a P-P bond and shifting a lone pair, thus perfectly balanced with respect to distorting toward either structure. As for the 1D Peierls chain,[41] a lattice vibration mode of symmetrical pairing of atoms is realized by two equivalent bond localization fashions (P-P P-P ↔ P·P·P·P· ↔ -P P-P P-).

The striking difference with respect to the Woodward-Hoffmann mechanism of Burdett[42] is the strictly local character[18,43] of the Peierls chain and bond flipping events. P-P bonds are interconverted into lone pairs and vice versa by local rules of homolytic bond breaking resulting into an instable chain at the interface between *A*17 and *A*7. Pressure literally squeezes electrons out of this van der Waals reservoir into the P-P bond scaffolding, under formation of a Peierls chain. Layered structures result from lone pair relocation into "empty" van der Waals regions.

To better capture the mechanism of bonds and lone pairs relocation, Wannier functions were calculated. The Fourier transform of Bloch states into Wannier functions is defined up to a phase factor. A unique set of maximally localized Wannier functions (MLWFs)[44] is obtained by minimizing the total quadratic spread of the Wannier orbitals, like implemented in the WANNIER90[45] program. For the MLWFs of Fig. 5 sp^3 projection functions were used. This choice consistently produces three "bonds" and one "lone pair" on phosphorus in *A*17 and *A*7. Like for the ELI analysis, the chain in the intermediate steps appear different. In compressed black phosphorus *A*17 (Fig. 5, $t = 0$ fs) a bond is clearly distinct from a lone pair. In the regime of rapid bond flipping, two equally spread and shaped MLWFs appear (Fig. 5, $t =$ 1920,1960 fs). In the *A*7 structure (Fig. 5, 3240 fs), the former bond has become a lone pair. Within the chain, a rapid change of spread and shape of MLWFs is the electronic signature of the reconstruction.

The short-lived P-P polymer locally appears when a fraction of one phase is converted into the other. A set of bond forming/bond breaking events may be as short as 40 ps. Concomitantly, lone pairs are reoriented while remaining stereochemically active during the transformation (Fig. 4). The

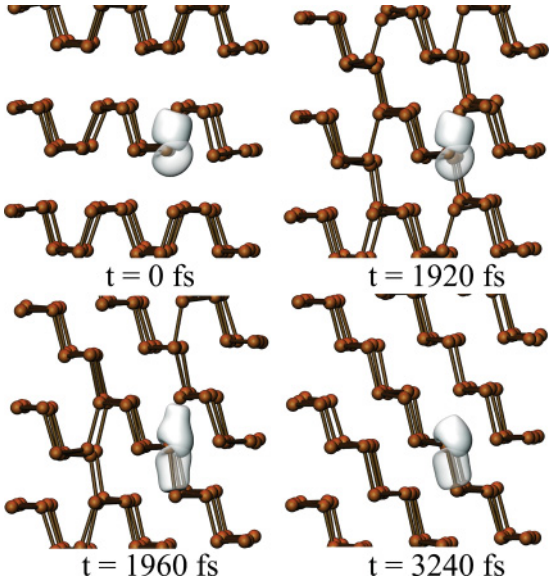

FIG. 5. (Color online) Bond-to-lone pair interconversion on a phosphorus atom illustrated with sp^3 projected MLWFs. A bond (opaque) and a lone pair (transparent) are represented in the $A17$ structure ($t = 0$ fs). The lone pair is closer to P but more spread out. In the intermediate configurations they become equal in size and shape. In the $A7$ structure the former bond has become a lone pair, and vice versa. Only the positive lobe of the MLWFs is rendered, for clarity.

different scales indicated above comprise an electronic step of chain formation and bond rearrangement at the interface (at constant volume), and a lock-in step into either $A7$ or $A17$, which is carried by a slower lattice dynamics along different distortion modes, under volume change. Distinct time scales are intrinsic to the process, as expected for a Peierls instability.

The chain collapse into $2c$-$2e$ bond sequences may take place with a more or less pronounced delay on the sequence of the events (Fig. 3), depending on the direction of the transformation. However, the glue for black phosphorus and As type to communicate in the intermediate (phase coexistence) region is over the polyradical, unstable chain. This is schematically represented in Fig. 6.

The lone pair reorientation leads to layer restacking and to a changed six-ring conformation. A correspondence can be made with molecular isomerization reactions. Like in the Cope rearrangement[46] (Fig. 1), an electronic effect leads to distinguishable configurations. For this molecular process, besides a concerted pericyclic process, an intermediate biradical mechanism is indicated.[47] For particular atomic assemblies, like in the P_7^{3-} anion, a degenerate Cope rearrangement leads to valence tautomerism.[48,49]

From the electronic count in the intermediate chain, a *polyradical* mechanism is proposed for the $A17 \rightarrow A7$ transition, as a solid-state version of the molecular Cope rearrangement. The coordination of P atoms in the chain is momentarily augmented from 3 to 4 under conservation of the lone pair stereoactivity. The resulting delocalization and possible distortion of the polymeric zigzag chain are summarized in Fig. 6.

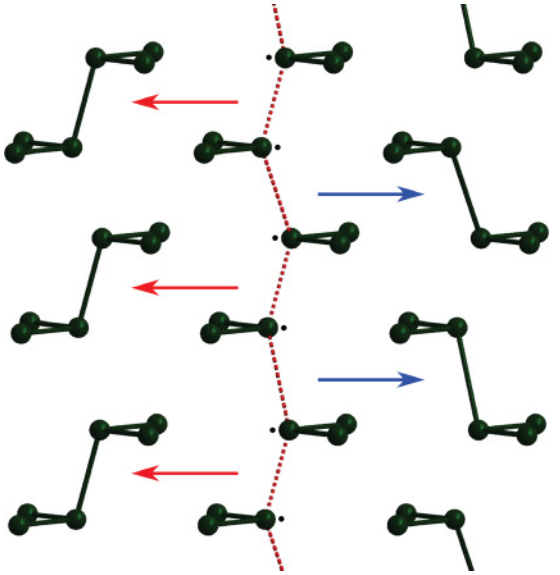

FIG. 6. (Color online) Schematic Cope-like mechanism for the $A17 \rightarrow A7$ transformation with a polyradical intermediate. Sets of arrows of different colors shows the distinguishable configurations resulting from shortening every other bond within the chain.

In Fig. 7, band structures[37] of intermediate configurations resulting from a collective bond-breaking, bond-formation pattern and from a TPS trajectory, respectively, are compared. The Brillouin-zone and special point symbols refer to the orthorhombic primitive cell of the *Pmna* subgroup of black phosphorus. In this primitive cell setting the stacking axis c of $A17$ runs along [001]. The bands are decorated with fat bands showing the contribution of p_z orbitals. In the concerted model bands cross between Y and Γ, at

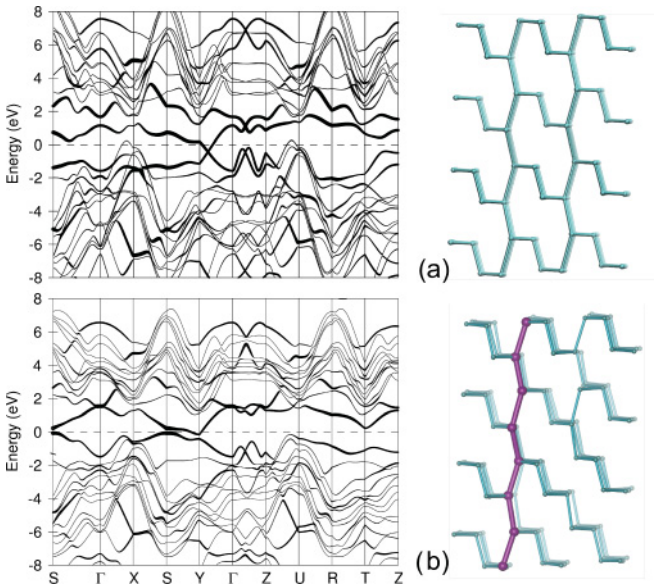

FIG. 7. (Color online) (a) Band structure of a symmetric intermediate from a concerted mechanism with bands crossing between Γ and Y. (b) Band structure (left) and configuration (right) of an intermediate resulting from TPS simulation. Band crossing is avoided. A cusp at S (b) and a cone between Y and Γ (a) are visible.

approximately 0.4 eV below the Fermi level. The region between X ($k = \frac{1}{2}; 0; 0$) and Y ($k = 0; \frac{1}{2}; 0$) through S ($k = \frac{1}{2}; \frac{1}{2}; 0$) shows reduced dispersion, almost flat-band character. In the nonconcerted version obtained from TPS, only at S ($k = \frac{1}{2}; \frac{1}{2}; 0$) is there a cusp in the DOS. The region between X and Y shows bands with reduced dispersion (flat bands), which are shifted just below the Fermi level by the distortion. We note similar band-structure features in a recent work.[50]

The Peierls distortion described by Burdett *et al.*[20,42] for the $A17 \rightarrow A7$ transformation based on an underlying α-Po pattern was a concerted process involving the whole material, as such even *forbidden* by the very same symmetry that made it possible. In the polyradical chain scenario lone pair and Peierls distortion are compatible features. The nonsimultaneous formation of polyradical chains avoids forbidden crossing and draws the line between the above-mentioned concerted models and our findings.

The Cope-like mechanism based on a polyradical intermediate provides a solution to the mentioned complications at least for three reasons: (a) it is a rapid electronic process taking place locally within the reconstruction propagation front, made of local bond flips correlated within a chain, (b) a low-dimensional interface is formed between different structural motifs along a noncontinuous, nonmartensitic process, where the bond switching is taking place, (c) lone pair rearrangement mechanisms and bond flipping pattern are geared together, which allows for both the formation of a 1D chain and the conservation of lone pair identities (as seen from the ELI map). The local character of the bond-forming, bond-breaking events releases many of the symmetry constraints of the concerted mechanism. In reciprocal space, while the latter causes bands to stick together at the high-symmetry point, degenerate states and band crossings can be avoided in the former (Fig. 7). Although challenging in principle, recent time-resolved electron imaging techniques may be appropriate to investigate electron density changes along the reaction coordinate.[51]

IV. CONCLUSIONS

Our analysis shows that black phosphorous and arsenic types are not just juxtaposed on the phase diagram, but tightly coupled. We predict the possibility of black phosphorus-type modification for the heavier elements As and Sb, for which the arsenic-type structure is the ground state. Increasing proximity of *s* and *p* states may impair black phosphorus formation in Bi. Since compression would lead to other compounds, we expect chemical routes over (Zintl phase) precursor decomposition to possibly achieve this.[52]

The precise atomistic picture and the evidence of a lower-dimensional intermediate in a region and on a time scale still inaccessible to experiments indicate a perspective of optimally combining computational and laboratory experiments. Along this way we are confident that novel insights can be provided into the fundamental problem of polymorphism, beginning with the (simple?) elements.

ACKNOWLEDGMENTS

We thank ZIH (TU Dresden) and NYBlue (NYCCS/BNL) for computational time. S.E.B. acknowledges DARPA (Grant No. 54751) for funding. S.L. thanks the DFG (Grant No. SPP 1415) for support. We are grateful to Michael Ruck for stimulating discussions. We thank Don Seo for critically reading the manuscript. Discussions with Carlo Gatti and Miroslav Kohout on ELF/ELI are gratefully acknowledged. S.L. wishes to thank Alexander Yaresko and Luis Craco for deep insights into band-structure calculations and electronic correlation effects, respectively.

*stefano.leoni@chemie.tu-dresden.de

[1] A. Pfitzner, Angew. Chem. Int. Ed. **45**, 699 (2005).
[2] M. Ruck, D. Hoppe, B. Wahl, P. Simon, Y. Wang, and G. Seifert, Angew. Chem. Int. Ed. **44**, 7616 (2005).
[3] J. Donohue, *The Structure of the Elements* (Robert E. Krieger, Malabar, FL, 1982).
[4] M. Marqués, G. J. Ackland, L. F. Lundegaard, S. Falconi, C. Hejny, M. I. McMahon, J. Contreras-Garcia, and M. Hanfland, Phys. Rev. B **78**, 054120 (2008).
[5] F. J. H. Ehlers and N. E. Christensen, Phys. Rev. B **69**, 214112 (2004).
[6] T. Ishikawa, H. Nagara, K. Kusakabe, and N. Suzuki, Phys. Rev. Lett. **96**, 095502 (2006).
[7] H. Fujihisa, Y. Akahama, H. Kawamura, Y. Ohishi, Y. Gotoh, H. Yamawaki, M. Sakashita, S. Takeya, and K. Honda, Phys. Rev. Lett. **98**, 175501 (2007).
[8] A. S. Mikhaylushkin, S. I. Simak, B. Johansson, and U. Häussermann, Phys. Rev. B **76**, 092103 (2007).
[9] R. Hultgren, N. S. Gingrich, and B. E. Warren, J. Chem. Phys. **3**, 351 (1935).
[10] A. Brown and S. Rundqvist, Acta Crystallogr. **19**, 684 (1965).
[11] J. C. Jamieson, Science **139**, 1291 (1963).
[12] R. Hoffmann, *Solids and Surfaces* (Wiley-VCH, New York, 1988).
[13] D.-K. Seo and R. Hoffmann, J. Solid State Chem. **147**, 26 (1999).
[14] J. K. Burdett and T. J. MacLarnan, J. Chem. Phys. **75**, 5764 (1981).
[15] J. K. Burdett, P. Haaland, and T. J. MacLarnan, J. Chem. Phys. **75**, 5774 (1981).
[16] U. Häussermann, Chem. Eur. J. **9**, 1471 (2003).
[17] H. Katzke and P. Tolédano, Phys. Rev. B **77**, 024109 (2008).
[18] J. P. Gaspard, A. Pellegatti, F. Marinelli, and C. Bichara, Philosophical Magazine B **77**(3), 727 (1998).
[19] P. Littlewood, J. Phys. C **13**, 4855 (1980).
[20] J. K. Burdett and S. Lee, J. Solid State Chem. **44**, 415 (1982).
[21] R. J. Gillespie, Angew. Chem. Int. Ed. **6**, 819 (1967).
[22] P. G. Bolhuis, C. Dellago, and D. Chandler, Faraday Discuss. **110**, 421 (1998).
[23] C. Dellago, P. G. Bolhuis, and P. L. Geissler, Lect. Notes Phys. **703**, 349 (2006).
[24] S. E. Boulfelfel, D. Zahn, Y. Grin, and S. Leoni, Phys. Rev. Lett. **99**, 125505 (2007).

[25]S. Leoni, R. Ramlau, K. Meier, M. Schmidt, and U. Schwarz, Proc. Natl. Acad. Sci. USA **105**, 19612 (2008).
[26]S. Leoni and S. E. Boulfelfel, in *Modern Methods of Crystal Structure Prediction*, edited by A. R. Oganov (Wiley, Berlin, 2010), p. 181.
[27]P. Minary, G. Martyna, and M. Tuckerman, J. Chem. Phys. **118**, 2510 (2003).
[28]D. Zahn and S. Leoni, Phys. Rev. Lett. **92**, 250201 (2004).
[29][http://cp2k.berlios.de] (2011).
[30]B. Aradi, B. Hourahine, and T. Frauenheim, J. Phys. Chem. A **111**, 5678 (2007).
[31]G. Seifert, D. Porezag, and T. Frauenheim, Int. J. Quantum Chem. **58**, 185 (1996).
[32]S. Sugai, T. Ueda, and K. Murase, J. Phys. Soc. Jpn. **50**, 3356 (1981).
[33]Y. Akahama, M. Kobayashi, and H. Kawamura, Solid State Commun. **104**, 311 (1997).
[34]T. Akai, S. Endo, Y. Akahama, K. Koto, and Y. Maruyama, High Press. Res. **1**, 115 (1989).
[35]M. Kohout, Int. J. Quantum Chem. **97**, 651 (2004).
[36]M. Kohout, Faraday Discuss. **135**, 43 (2007).
[37]O. Jepsen and O. K. Andersen, *The Stuttgart TB-LMTO Program (Version 4.7)* (MPI FKF, Stuttgart, 2000).
[38]A. I. Baranov and M. Kohout, J. Phys. Chem. Solids **71**, 1350 (2010).
[39]J. F. Dobson, J Chem. Phys. **94**, 4328 (1991).
[40]M. Kohout, *Program DGRID (Version 4.5)* (Radebeul, 2010).
[41]R. E. Peierls, *Quantum Theory of Solids* (Oxford University Press, London, 1955).
[42]J. K. Burdett and S. L. Price, Phys. Rev. B **25**, 5778 (1982).
[43]M.-H. Whangbo, J. Chem. Phys. **75**, 4983 (1981).
[44]N. Marzari and D. Vanderbilt, Phys. Rev. B **56**, 12847 (1997).
[45]A. A. Mostofi, J. R. Yates, Y.-S. Lee, I. Souza, D. Vanderbilt, and N. Marzari, Comput. Phys. Commun. **178**, 685 (2008).
[46]A. C. Cope and E. M. Hardy, J. Am. Chem. Soc. **62**, 441 (1940).
[47]J. A. Berson and M. Jones Jr., J. Am. Chem. Soc. **86**, 5017 (1964).
[48]C. Jäger, D. Reichert, H. Zimmermann, T. Sen, R. Poupko, and Z. Luz, J. Magn. Reson. **153**, 227 (2001).
[49]G. Seifert and R. O. Jones, J. Chem. Phys. **96**, 2951 (1992).
[50]G. Bihlmayer, Y. Koroteev, and E. Chulkov, New J. Phys. **12**, 065006 (2010).
[51]A. H. Zewail, Science **328**, 187 (2010).
[52]A. M. Guloy, R. Ramlau, Z. Tang, W. Schnelle, M. Baitinger, and Y. Grin, Nature (London) **443**, 320 (2006).